

# Energy extrema and Nonlinear Stability in a Variational theory of Barotropic Flow on a Rotating Sphere

Chjan C. Lim

Mathematical Sciences, RPI, Troy, NY 12180, USA

email: lim@rpi.edu

March 20, 2019

## Abstract

The main result is that at any rate of spin and relative enstrophy  $Q_{\text{rel}}$ , the unique global energy maximizer for fixed relative enstrophy corresponds to solid-body rotation,  $w_{\text{Max}}^0(Q_{\text{rel}}) = \frac{p}{Q_{\text{rel}}^{1/2}}$  in the direction of spin. Another solution, the counter-rotating steady-state  $w_{\text{min}}^0(Q_{\text{rel}}) = \frac{p}{Q_{\text{rel}}^{1/2}}$ , is a constrained energy minimum provided the relative enstrophy is small enough, i.e.,  $Q_{\text{rel}} < C^2$  where  $C = j \cos \beta$ . If  $C^2 < Q_{\text{rel}}$ , then  $w_{\text{min}}^0(Q_{\text{rel}})$  is a saddle point.

For all energy  $H$  below a threshold value  $H_c$  which depends on the relative enstrophy  $Q_{\text{rel}}$  and spin, the constrained energy extrema consist of only minimizers and saddles in the form of counter-rotating states,  $\frac{p}{Q_{\text{rel}}^{1/2}}$ . Only when the energy exceeds this threshold value  $H_c$ , can pro-rotating states,  $\frac{p}{Q_{\text{rel}}^{1/2}}$  arise as global maximizers.

Given the conditions for  $w_{\text{min}}^0(Q_{\text{rel}})$  to be a local constrained minimum, the solid-body rotation opposite to spin  $w_{\text{min}}^0(Q_{\text{rel}})$  is nonlinearly stable. The global constrained maximizer  $w_{\text{Max}}^0(Q_{\text{rel}})$  corresponding to solid-body rotation in the direction of spin, is always nonlinearly stable.

# 1 Introduction

The main aim of this paper is to present the simplest possible formulation and rigorous analysis of a theory for geophysical flow on the rotating sphere, which exhibits characteristics of super and sub-rotation. We do not claim that our theory and results explain the complex range of phenomena associated with super-rotation such as pertaining to the Venusian atmosphere (cf. [12] and references therein). The starting point of much of that body of work is a multi-layer stratified rotating flow model. Furthermore, the system modelled is usually a dammed driven one with differential solar radiation and Ekman damping. The best results to date are therefore based on numerically intensive simulations using the General Circulation Model (GCM). Although the GCM simulations reproduced some aspects of super-rotation such as those on Venus and Titan, a rigorous theory which can be analysed in classical mathematical terms, is lacking. This is the motivation which guides our approach here.

We therefore propose a mathematically precise constrained variational problem in terms of the pseudo energy (total kinetic energy) of barotropic flow on a rotating sphere, in which the only explicit constraints are fixed relative enstrophy and zero total circulation. Unlike previous work, the angular momentum is not fixed. This is a necessary condition for atmospheric super-rotation as the most promising theory to date is one where the rotating atmosphere exchanges angular momentum with the planetary surface through a complex torque mechanism.

The main results of this approach is that, at any rate of spin and relative enstrophy  $Q_{\text{rel}}$ , the constrained global energy maximum for fixed relative enstrophy corresponds to solid-body rotation,  $w_{\text{Max}}^0(Q_{\text{rel}}) = \sqrt{\frac{Q_{\text{rel}}}{10}}$ ; in the direction of  $\hat{p}$ : Another solution, the counter-rotating steady state  $w_{\text{min}}^0(Q_{\text{rel}}) = \sqrt{\frac{Q_{\text{rel}}}{10}}$ ; is a constrained global energy minimum provided the relative enstrophy is small enough, that is,  $Q_{\text{rel}} < 2C^2$  where  $C = j\cos\tilde{\theta}$ : If  $2C^2 < Q_{\text{rel}} < 4C^2$ ; then  $w_{\text{min}}^0(Q_{\text{rel}})$  is a saddle point. And if  $Q_{\text{rel}} > 4C^2$ ; then  $w_{\text{min}}^0(Q_{\text{rel}})$  is again a saddle point, but in the restricted sense that it is a constrained local energy maximum in all eigen-directions except  $_{1,1}$ ;  $w_{\text{min}}^0(Q_{\text{rel}})$  is a constrained local energy minimum in the projection onto  $\text{span}(\hat{p}_{10}, \hat{p}_{1,1})$  where the  $_{1,1}$  eigenmodes are relative vorticity

patterns associated with the tilt instability.

The main result can be viewed another way. For all energy  $H$  below a threshold value  $H_c$  which depends on the relative enstrophy  $Q_{\text{rel}}$  and spin ; the constrained energy extremals consist of only minima and saddles in the form of counter-rotating states,  $\overline{Q_{\text{rel}}}_{10}^p$ : Only when the energy exceeds this threshold value  $H_c$ , can pro-rotating states,  $\overline{Q_{\text{rel}}}_{10}^p$  arise as constrained global energy maxima.

It is useful to view the approach in this paper in the light of a vertically coarse-grained variational analysis of the steady states of the barotropic component of the actual fully stratified rotating flows. We recall another robust connection between the time-independent variational theory presented and dynamical initial value problems for dam-ped driven quasi-geostrophic flows: the Principle of Selective Decay or Minimum Enstrophy states that, for suitable initial data, the long time asymptotics of the 2D Navier-Stokes equations on a doubly-periodic domain (and by extension the sphere), is characterized by a decreasing enstrophy to energy ratio [5]. These Minimum Enstrophy flows are characterized by special steady states which are the solid body rotational flows in the case of the sphere, by virtue of an application of Poincaré's Inequality [21]. In 1953, Fjørtoft [7] used a spherical harmonics expansion to show that, for the dissipative BVE, because the enstrophy spectrum is related to the energy spectrum by  $Z(l;t) = l(l+1)E(l;t)$ , the energy fluxes towards low wavenumbers  $l$  while enstrophy fluxes towards high  $l$  modes. His work is influential in bringing forth the concepts of the inverse cascade of energy and forward cascade of enstrophy that are closely related to Selective Decay.

Indeed, an inviscid asymptotic formulation of the Principle of Minimum Enstrophy yields a variational problem that is the dual of the one in this paper, namely, extremize enstrophy at fixed values of the total kinetic energy of flow. The corresponding extremals including states of minimum enstrophy are again solid-body rotating flows. Leith [8] formulated this method precisely by looking for constrained enstrophy extremals in vortex dynamics with either fixed kinetic energy or angular momentum.

Stability results for barotropic flows are discussed in Fjørtoft [6], Tung [20], and Shepherd et al [2], [9] amongst many others. Fjørtoft [6] first used integral theorems to argue that solid-body rotational flows are stable in the BVE context although it was Arnold [10], [11] who formalized this body of results known as the energy-Casimir method, and proved that they work at finite amplitudes, that is in a nonlinear way. According to an argument of

Shepherd [1], the Lyapunov function method fails precisely when the planetary spin  $\Omega$  is small (cf. also the note by Wirosoetisno and Shepherd [9] which proved that there are two important cases in 2D Euler flows where the Arnold stability method fails, and one of them is the non-rotating sphere). Our result on the instability of the retrograde (east to west) solid-body flow is compatible with Shepherd's precisely because we proved instability only when the planetary spin  $\Omega$  is smaller than  $\Omega_{\text{rel}} = C^2$ : Indeed, our result also states that when  $C^2 > \Omega_{\text{rel}}$  (large enough planetary spins), both prograde and retrograde rigid rotations are nonlinearly stable.

In section 2 we give the barotropic vorticity equation and its conserved quantities, as useful background for the rest of the paper although the initial value problem for this equation is not relevant to the discussion. Section 3 describes the energy-enstrophy class of variational formulations for the relaxed-BVE, which we shall call BVE-related models in this paper: Section 4 gives the constrained optimization of flow energy,  $H$  on fixed relative enstrophy manifolds and section 5 describes the physical characteristics of the constrained energy extrema that arise in the BVE-related models. Section 6 gives the nonlinear stability results. Section 7 concerns physical consequences.

## 2 Barotropic Vorticity Model (BVE)

After identifying the PDE model (BVE) to use at the start of our investigation, there remains, however, several intermediate steps before a successful variational formulation can be derived. This is due to the goals we have set, namely, to derive and prove rigorous results which state explicitly verifiable conditions for super and sub-rotation within the BVE. Another related reason is the fact that the initial value problem for the BVE is far too complex for our purposes, although it is well suited to numerical studies. In a nutshell, we need to find a suitable set of constraints for the obvious choice of objective functional, namely total kinetic energy of flow in the BVE. The choice of auxiliary conditions or constraints is not a priori obvious, as different choices can have slightly different physical consequences [22].

In spherical coordinates ( $\cos \theta$  where  $\theta$  is the colatitude; longitude  $\phi$ ); the barotropic vorticity equation (BVE) is

$$\mathbf{q}_t + \mathbf{J}(\mathbf{q}; \mathbf{q}) = 0 \quad (1)$$

$$q(t; \cos \phi) = \dots + 2 \cos$$

where  $q$  is the total vorticity,  $2 \cos$  is the planetary vorticity due to spin rate and  $w = \dots$  is the relative vorticity given in terms of a relative velocity stream function and  $\Delta$  is the negative of the Laplace-Beltrami operator on the unit sphere  $S^2$ :

The symmetries of the problem on the rotating sphere differ from that on the non-rotating sphere: The former is  $SO(2)$  symmetric and the latter is  $SO(3)$  symmetric. Although the  $\phi = 0$  case is  $SO(3)$  symmetric, it is known that certain constrained global energy maximizers are robust symmetry-breaking steady states in the problem with no rotation [15].

## 2.1 Steady states

Steady states of the BVE are easily characterized: let  $q = q(\phi)$  be any smooth function of the relative stream function  $\phi$ , then any solutions of the following nonlinear elliptic PDE,

$$\begin{aligned} \frac{1}{2} \int_{S^2} 2 \cos \phi \Delta q(\phi) &= q(\phi) \\ \int_{S^2} dx &= 0; \end{aligned}$$

is a steady state relative stream function in the sense that the relative vorticity  $w = \dots$  is a time independent solution of the BVE. This can be easily seen by setting the Jacobian in (1) to zero (cf. [?]) and also [13]). In particular, any zonal stream function  $\phi = \phi(\phi)$  represents a steady state solution of the BVE.

## 2.2 Inverse of the Laplacian

Key to the analysis below is the inverse integral operator defined by

$$G[f](x) = \frac{1}{2} \int_{S^2} dx^0 f(x^0) \ln \frac{1}{|x - x^0|}$$

on  $S^2$ : In terms of  $G$ ; the solution of

$$\Delta f(x) = f(x)$$

is given by

$$\begin{aligned} (x) &= \int_0^1 (f) = G[f](x) \\ &= \frac{1}{2} \int_{S^2} dx^0 f(x^0) \ln \frac{1}{|x - x^0|}: \end{aligned}$$

Given the total vorticity  $q$  satisfying the zero circulation condition  $\int_R q dx = 0$ , we solve

$$= q = 2 \cos$$

for the relative stream function

$$\begin{aligned} &= G[q] = 2 \cos \\ &= \frac{1}{2} \int_{S^2} dx^0 [q(x^0) = 2 \cos] \ln \frac{1}{|x - x^0|} \\ &= G[q] = 2 G[\cos]: \end{aligned}$$

The last equality follows from the linearity of  $G$ :

### 2.3 Eigenfunctions of $G$

The variational analysis of this problem is based on the fact that there is an orthonormal basis for  $L^2(S^2)$  of eigenfunctions of the Laplace-Beltrami operator and  $G$ ; consisting of the spherical harmonics,

$$\begin{aligned} l_m; m &= 1, \dots, l \\ \text{which have eigenvalue } l_m &= l(l+1): \end{aligned} \tag{2}$$

### 2.4 Conserved quantities of the barotropic vorticity model

The barotropic vorticity model conserves the kinetic energy and any function of the vorticity are conserved as the governing equation. For a survey of recent work on the Hamiltonian approach to geophysical problems, we recommend Shepherd's [?]. The total kinetic energy

$$\begin{aligned} H_T[q] &= \frac{1}{2} \int_{S^2}^Z dx^h (u_r + u_p)^2 + v_r^2 \\ &= \frac{1}{2} \int_{S^2}^Z dx^h (u_r^2 + v_r^2) + 2u_r u_p + \frac{1}{2} \int_{S^2}^Z dx^i u_p^2 \\ &= \frac{1}{2} \int_{S^2}^Z dx^i q + \frac{1}{2} \int_{S^2}^Z dx^i u_p^2 \end{aligned}$$

where  $u_r, v_r$  are the zonal and meridional components of the relative velocity,  $u_p$  is the zonal component of the planetary velocity (the meridional component being zero since planetary vorticity is zonal), and  $\psi$  is the stream function for the relative velocity.

Since the second term  $\frac{1}{2} \int_{S^2} dx u_p^2$  is fixed for a given spin rate  $\Omega$ ; it is convenient to work with the conserved pseudo-energy as the Hamiltonian functional for the BVE, i.e.,

$$\begin{aligned} H[\mathbf{q}] &= \frac{1}{2} \int_{S^2} dx \mathbf{q} \cdot \mathbf{q} = \frac{1}{2} \int_{S^2} dx [w(x) + 2 \cos \phi] \\ &= \frac{1}{2} \int_{S^2} dx [w(x)w(x) + 2 \cos \phi \cos \phi] \\ &= \frac{1}{2} h w ; G[w] + C h_{10} ; G[w] \end{aligned}$$

where  $C = \int_0^{\pi} \int_0^{2\pi} \cos^2 \phi d\phi d\theta$ ;

$$KE_{\text{rel}} = \frac{1}{2} \int_{S^2} dx [w(x)w(x)] = \frac{1}{2} h w ; G[w]$$

is the pseudo-kinetic energy of relative motion and

$$C h_{10} ; G[w]$$

is that part of the total kinetic energy arising from the interaction between relative vorticity  $w$  and planetary vorticity  $2 \cos \phi$ : It will be convenient to perform one more minor adjustment of the Hamiltonian functional in Lemma 3 to turn it into a positive definite quadratic form in the Fourier coefficients of the spectral expansion of the relative vorticity  $w$  in the spherical harmonics

in :

After the fixed total circulation  $\int_{S^2} \mathbf{q} \cdot d\mathbf{x} = \int_{S^2} w d\mathbf{x} = 0$ ; the next important conserved vorticity moment is the total enstrophy

$$[\mathbf{q}] = \int_{S^2} dx \mathbf{q}^2$$

One reason that the enstrophy is important follows from the fact that it is just the  $L^2$  norm of the total vorticity  $\mathbf{q}$ ; and it is natural to work in the Hilbert space,  $L^2(S^2)$ : Expanding (cf. [1]),

$$\begin{aligned} [\mathbf{q}] &= \int_{S^2} dx \mathbf{q}^2 = \int_{S^2} dx [w + 2 \cos \phi]^2 \\ &= \int_{S^2} dx w^2 + 4 \int_{S^2} dx w \cos \phi + 4 \int_{S^2} dx \cos^2 \phi; \end{aligned} \tag{3}$$

we find that the last term is a conserved quantity because it is the square of the  $L^2$  norm of the fixed planetary vorticity, the second term is Kelvin's conserved impulse and thus, the first term which is the square of the  $L^2$  norm of the relative vorticity, is a conserved quantity. The conservation of the second term follows also from the fact that it is the axial component of the "angular momentum" of the relative vorticity. The conservation of this "angular momentum" follows from an application of Noether's theorem on the basis that the barotropic vorticity equation is  $SO(2)$  invariant with respect to distinguished direction corresponding to the spin :

The second term in (3) is equal to 4 times the angular momentum density of the relative uid motion and has units of  $m^4/s$ . The physical angular momentum, given by

$$\int_S w \cos \theta \, d\Omega = h w \cos i; \quad (4)$$

implies that the only mode in the eigenfunction expansion of  $w$  that contributes to the angular momentum is  $Y_{10}$  where  $Y_{10} = a \cos \theta$  is the first nontrivial spherical harmonic; it has the form of solid-body rotation vorticity.

All other moments of the vorticity  $\int_S w^n \cos \theta \, d\Omega$  are conserved but are deemed less important in many physical theories of uid motions including the absolute equilibrium statistical mechanics model [14] and the variational problems below [16]. They are, however, not totally irrelevant [22].

### 3 Energy-relative enstrophy variational theory

The Lagrange Multiplier method for Hilbert space [19] gives necessary conditions for constrained extremals in the form of Euler-Lagrange equations. More importantly, the explicit form of the Lagrange Multipliers in terms of spin, energy and relative enstrophy, provides the detailed physical relationships that we seek in order to answer the questions raised. We also extend the Lagrange Multiplier method to give a geometrical proof of the existence and nonlinear stability of the constrained energy extremals in the BVE where the constraint is fixed relative enstrophy.

Not only are the higher vorticity moments  $\int_S w^n \cos \theta \, d\Omega$  for  $n > 2$  ignored in this paper (cf. also [14]. We also do not constrain the total enstrophy

$$\int_S w^2 \, d\Omega + 4 \int_S w \cos \theta \, d\Omega$$

nor the angular momentum

$$\int_{S^2} dx w \cos \phi : \quad (5)$$

The only constraint in this paper besides the zero total circulation condition,

$$\int_{S^2} dx w = 0; \quad (6)$$

is that the relative enstrophy,

$$\int_{S^2} dx w^2 = Q_{\text{rel}} > 0; \quad (7)$$

is fixed.

### 3.1 Constraint $V_{\text{rel}}$

We first analyze the physical consequences of the constraint  $\int_{S^2} dx w^2 = Q_{\text{rel}} > 0$  in the definition of the subset

$$V_{\text{rel}} = \{ w \in L^2(S^2) \mid \int_{S^2} dx w^2 = Q_{\text{rel}} > 0; \text{TC} = \int_{S^2} dx w = 0 \};$$

which leave the angular momentum (5) constrained only by an inequality. Fixing the relative enstrophy and relative circulation, this model allows in principle energy extrema which can have up to a maximum amount of super or sub-rotation. It has the interesting consequence that angular momentum is effectively constrained by an inequality.

**Lemma 1:** Let the circulation and relative enstrophy of  $w \in L^2(S^2)$  be constrained by (6) and (7) respectively. Then, the angular momentum (5) is constrained by an inequality, that is,

$$\int_{S^2} dx w \cos \phi \leq C \frac{Q_{\text{rel}}}{\sqrt{Q_{\text{rel}}}} \quad (8)$$

where  $C > 0$  is a constant that does not depend on  $w$ :

**Proof:** By the Cauchy-Schwartz inequality [21], the result is proved with

$$C^2 = \int_{S^2} (\cos \phi)^2 dx : \quad (9)$$

QED.

It is not surprising that solid-body rotation vorticity in the form of spherical harmonic  $\psi_{10} = b \cos \theta$  is the only zero circulation relative vorticity field that maximizes angular momentum for given enstrophy. This is stated precisely below :

**Lemma 2:** The upper bound on the angular momentum in (8) is achieved only for relative vorticity field

$$w = k \cos \theta$$

where  $k$  is a constant.

**Proof:** When  $w = k \cos \theta$  ;

$$\int_{S^2} d\theta d\phi w \cos \theta = \int_{S^2} d\theta d\phi k \cos^2 \theta = k C^2$$

and

$$\int_{S^2} d\theta d\phi w^2 = k^2 C^2 = Q_{\text{rel}}$$

Thus,

$$\int_{S^2} d\theta d\phi w \cos \theta = C \frac{Q_{\text{rel}}}{C}$$

Conversely, if

$$w = k \cos \theta + a \sin \theta$$

where  $a \neq 0$  and  $a \neq 0$ ; then

$$\int_{S^2} d\theta d\phi w \cos \theta < C \int_{S^2} d\theta d\phi w^2$$

QED .

### 3.2 Augmented energy functionals

The unconstrained optimization of the augmented energy-relative enstrophy functional arising from the Lagrange Multiplier method yield necessary conditions for extremals of the constrained optimization problems. Necessary conditions for the extremals of the augmented functionals are in turn given in terms of their Euler-Lagrange equations (or Gateaux derivative) which take the form of interesting inhomogeneous linear equations involving the inverse  $G$  of the Laplace-Beltrami operator. Bifurcation values of the multipliers can be read off the spectrum of  $G$ . Extremals of the augmented

energy functional typically change type for different regimes of the Lagrange multiplier values which are marked by bifurcation values.

The relative enstrophy constraint gives rise to the following constrained optimization problems:

$$\text{extreme } H[w] \text{ on } \mathcal{Z} \quad (10)$$

$$V_{\text{rel}} = \frac{1}{2} \int_{\mathcal{S}^2} w \cdot \nabla^2 w \cdot \nabla w = \int_{\mathcal{S}^2} \nabla w \cdot \nabla w = Q_{\text{rel}} > 0; \quad \int_{\mathcal{S}^2} dx w = 0 \quad (11)$$

By the method of Lagrange Multipliers (see [19], [18]), the energy-relative enstrophy functional

$$E_{\text{rel}}[w; \lambda; R] = H[w] + \lambda \int_{\mathcal{S}^2} w \cdot \nabla w \quad (12)$$

is the augmented objective functional for the unconstrained optimization problem corresponding to the above constrained optimization problem.

### 3.3 Lagrange Multipliers

The Euler-Lagrange Multiplier theorem states: Let  $w_0 \in V_{\text{rel}}$  be an extremal of  $H[w]$ . Then at least one of the following holds:

$$(1) \quad \lambda_{\text{rel}}(w_0) = 0;$$

$$(2) \quad E_{\text{rel}}(w_0) = H(w_0) + \lambda_{\text{rel}}(w_0) = 0;$$

The right way to use this theorem is: (a) find a set of relative vorticity  $w \in V_{\text{rel}}$  which satisfies  $\lambda_{\text{rel}}(w) = 0$ ; (b) find a second set of relative vorticity  $w \in V_{\text{rel}}$  which satisfies  $H(w) + \lambda_{\text{rel}}(w) = 0$ ; for some  $\lambda$ ; (c) the set of constrained extremals of  $H[w]$  is contained in the union of the sets in (a) and (b), and (d) the value of  $\lambda$  is determined from the value of the fixed constant  $\lambda_{\text{rel}}(w) = Q_{\text{rel}} > 0$ :

In implementing this procedure we first compute the variation or Gateaux derivative

$$\lambda_{\text{rel}}(w; \tilde{w}) = 2 \int_{\mathcal{S}^2} w \cdot \nabla \tilde{w} dx;$$

By choosing  $\tilde{w} = w$ ; we show that this variation never vanishes for any  $w$ ; i.e.,

$$(1) \quad \lambda_{\text{rel}}(w) \neq 0;$$

The Euler-Lagrange Multiplier theorem then states that any extremal  $w_0$  of the constrained variational problem (10) and (11) must satisfy

$$(2) \quad E_{\text{rel}}(w_0) = H(w_0) + \lambda_{\text{rel}}(w_0) = 0$$

for some value of  $\lambda$ :

The vanishing of the Gâteaux derivative of the augmented functional  $E_{\text{rel}}$  gives the Euler-Lagrange equation for the unconstrained problem, which is solved in the next section.

#### 4 Extremals of the augmented energy functional

The analysis below will be based on the spherical harmonics (2) which are eigenfunctions of the Laplace-Beltrami operator on the sphere. In particular, the eigenfunction  $Y_{10} = \sqrt{3} \cos \theta$  which has eigenvalue  $\lambda_{10} = -2$ ; will play a special role in the characterization of the zonal steady states of the BVE. Using the linearity of  $G$ ; and the eigenfunction expansion

$$w = \sum_{l=1}^{\infty} \sum_{m=-l}^l c_{lm} Y_{lm}; \quad (13)$$

of relative vorticity  $w$  satisfying  $\int_{S^2} dx w = 0$ ; the Hamiltonian functional is expanded in terms of the orthonormal spherical harmonics, to yield

$$\begin{aligned} H &= \frac{1}{2} \int_{S^2} d\omega ; G[w] + C h_{10} ; G[w] \\ &= \frac{1}{2} \sum_{l=1}^{\infty} \sum_{m=-l}^l \frac{c_{lm}^2}{m} + \frac{1}{2} C h_{10}; \end{aligned} \quad (14)$$

It follows that the coupling between the relative motion and the planetary vorticity occurs through the eigenfunction  $Y_{10}$ ; which has the form of a vorticity pattern corresponding to solid-body rotational flow.

For obvious technical reasons, and without loss of generality, we will use the following lemma to change the Hamiltonian by a constant to a quadratic form.

Lemma 3: For fixed spin  $\omega > 0$ ; the energy  $H$  for  $w$  satisfying

$$\int_{S^2} dx w(x) = 0;$$

is modulo the constant

$$H_0 = \frac{1}{4} \mathbf{C}^2; \quad (15)$$

equal to the positive definite quadratic form (which we will again denote by  $H$ )

$$H = \frac{1}{4} [\mathbf{1}_{10} - (\mathbf{C})]^2 + \frac{1}{4} \mathbf{C}^2 + \frac{1}{2} \mathbf{x}^T \frac{1}{2} \mathbf{I}_{10} \mathbf{x} - \frac{1}{2} \mathbf{x}^T \frac{1}{2} \mathbf{I}_{10} \mathbf{x} = \frac{1}{2} \mathbf{x}^T \frac{1}{2} \mathbf{I}_{10} \mathbf{x}; \quad (16)$$

Proof: By completing the square,

$$\begin{aligned} H &= \frac{1}{2} \mathbf{x}^T \frac{1}{2} \mathbf{I}_{10} \mathbf{x} + \frac{1}{2} \mathbf{C}^T \mathbf{1}_{10} \\ &= \frac{1}{4} \mathbf{1}_{10}^T + \frac{1}{2} \mathbf{C}^T \mathbf{1}_{10} - \frac{1}{2} \mathbf{x}^T \frac{1}{2} \mathbf{I}_{10} \mathbf{x} \\ &= \frac{1}{4} \mathbf{1}_{10}^T + 2 \mathbf{C}^T \mathbf{1}_{10} + \frac{1}{4} \mathbf{C}^2 + \frac{1}{4} \mathbf{1}_{10}^T + \frac{1}{2} \mathbf{x}^T \frac{1}{2} \mathbf{I}_{10} \mathbf{x} - \frac{1}{4} \mathbf{C}^2 \\ &= \frac{1}{4} [\mathbf{1}_{10} - (\mathbf{C})]^2 + \frac{1}{4} \mathbf{C}^2 + \frac{1}{2} \mathbf{x}^T \frac{1}{2} \mathbf{I}_{10} \mathbf{x} - \frac{1}{4} \mathbf{C}^2; \end{aligned}$$

QED.

Since all the extrema  $\mathbf{w}^0$  below have the form  $\mathbf{k}_{10}$  of solid-body rotation, it is useful to state the following result. The simple proof is left to the reader. Graphs of (17) and (18) are depicted in figures 1 and 2.

Lemma 4: The energy and relative enstrophy of the extrema  $\mathbf{w}^0 = \mathbf{k}_{10}$  takes the form

$$\begin{aligned} H[\mathbf{k}_{10}] &= \frac{1}{4} (\mathbf{k}_{10} - \mathbf{C})^2 \\ Q_{\text{rel}} &= \frac{1}{2} \mathbf{k}_{10}^T \mathbf{k}_{10}; \end{aligned} \quad (17)$$

Furthermore, for fixed  $H$ ;

$$Q_{\text{rel}} = \frac{1}{2} \mathbf{C}^T \frac{Q}{Q_{\text{rel}}} + \frac{1}{4} \mathbf{C}^2 = 4H \quad (18)$$

with solutions

$$Q_{\text{rel}} = \mathbf{C}^T \mathbf{C} + \frac{p}{4H} \mathbf{C}^2; \quad (19)$$

## 4.1 Lagrange Multipliers

This constrained variational model is based on the fixed relative enstrophy constraint  $V_{\text{rel}}$ : By a theorem in [19] on the Lagrange Multiplier method, the variational problem (10), (11) can be reformulated in terms of extremes of the augmented functional,

$$\begin{aligned} E_{\text{rel}}[w; \lambda] &= H_{\bar{Z}}[w] + \lambda_{\text{rel}} V_{\text{rel}}[w]; \\ \lambda_{\text{rel}}[w] &= \frac{w^2 dx}{S^2}; \end{aligned}$$

Expanding  $\lambda_{\text{rel}}[w]$  in terms of (13) and combining with (16) yields

$$E_{\text{rel}}[w; \lambda] = \frac{1}{4} [ \frac{1}{10} ( -C ) ]^2 + \frac{1}{4} \sum_{i=1}^h \sum_{m=1}^{2i} \frac{1}{2} \frac{x}{2 \Delta x_m} \frac{\frac{2}{m}}{\frac{1}{m}} + \lambda_{\text{rel}} \sum_{i=1}^h \sum_{m=1}^{2i} \frac{x}{2 \Delta x_m} : \quad (20)$$

Taking the Gâteaux derivative of  $E_{\text{rel}}[w; \lambda]$  wrt  $w$  gives the Euler-Lagrange equation,

$$[G - 2 \lambda_{\text{rel}}](w^0) = \frac{1}{2} C_{10} : \quad (21)$$

By the Fredholm Alternative [21], equation (21) either (a) has solutions for all values of the right hand side, or (b) has infinite number of solutions when the right hand side is orthogonal to the kernel of  $[G - 2 \lambda_{\text{rel}}]$ : All the eigenvalues of  $G$  are negative and form an increasing sequence,  $\frac{1}{m}$ : There are several subcases, namely, (1)  $\lambda_{\text{rel}} = 2 \left( 1; \frac{1}{4} \right)$ ; (2)  $\lambda_{\text{rel}} = 2 \left( \frac{1}{4}; 1 \right)$ ;  $\lambda_{\text{rel}} \notin \frac{1}{21(1+1)}$  and (3)  $\lambda_{\text{rel}} = \frac{1}{21(1+1)} 2 \left[ \frac{1}{4}; 0 \right]$ ; which fall into the two broader classes that depend on whether or not the kernel of  $[G - 2 \lambda_{\text{rel}}]$  is trivial.

Although the results in the following theorem clearly have physical significance, they are nonetheless easy to establish because the Euler-Lagrange equation (21) is a linear equation. Figure 4 shows plots of (22) and (23).

Theorem 5:

- (1) Only when  $\lambda_{\text{rel}} = 2 \left( 1; \frac{1}{4} \right)$ ; can extremal relative vorticity in the form of solid-body rotation in the same direction as planetary vorticity arise;
- (2) For  $\lambda_{\text{rel}} = 2 \left( \frac{1}{4}; 1 \right)$ ;  $\lambda_{\text{rel}} \notin \frac{1}{21(1+1)}$ ; the extremal vorticity (if it exists), is solid-body rotation in the opposite direction as planetary vorticity;
- (3) Only when  $\lambda_{\text{rel}} = \frac{1}{21(1+1)} 2 \left[ \frac{1}{4}; 0 \right]$ ; can higher spherical harmonics  $\lambda_m$ ;  $m \neq 10$ ; contribute to the extremal vorticity.

The proof is divided into two natural subcases, namely, (a) when the kernel of  $[G - 2_{\text{rel}}]$  is empty, and (b) when it is not.

(a i)  $\text{rel} \geq 2 \left( 1 ; \frac{1}{4} \right)$

In this regime, the kernel of  $[G - 2_{\text{rel}}]$  is also empty, which implies the results:

$$\text{for } \text{rel} \geq 2 \left( 1 ; \frac{1}{4} \right); w^0 = \frac{C}{2 \frac{1}{2} + 2_{\text{rel}}} \cdot 1_0; \quad (22)$$

and,

$$\begin{aligned} w^0 &= k \cdot 1_0 \text{ with } k \neq 0^+ \text{ as } \text{rel} \neq 1; \\ w^0 &= k \cdot 1_0 \text{ with } k \neq 1 \text{ as } \text{rel} \neq \frac{1}{4}; \end{aligned}$$

Thus, there is a pole-like singularity at  $\text{rel} = 1$ : This proves part (1) of the theorem.

(a ii)  $\text{rel} \geq 2 \left( \frac{1}{4}; 0 \right)$  and  $\text{rel} \neq \frac{1}{2l(l+1)}$

In this case, the following holds:

$$\begin{aligned} \text{for } \text{rel} \geq 2 \left( \frac{1}{4}; 0 \right); \text{rel} \neq \frac{1}{2l(l+1)}; \\ w^0 = \frac{C}{2 \frac{1}{2} + 2_{\text{rel}}} \cdot 1_0; \end{aligned} \quad (23)$$

(a iii)  $\text{rel} < 0$

Since all eigenvalues of  $G$  are negative, the kernel of  $[G - 2_{\text{rel}}]$  is empty for  $\text{rel} > 0$ : Thus, the solution of (21) is easily found by setting  $w^0 = k \cdot 1_0$ :

$$k = \frac{C}{(1 + 4_{\text{rel}})};$$

This implies the result:

$$\begin{aligned} w^0 &= k \cdot 1_0 \text{ with } k \neq 0 \text{ as } \text{rel} \neq 1; \\ w^0 &= C \cdot 1_0 \text{ as } \text{rel} = 0^+; \end{aligned}$$

The special solution  $w^0 = C \cdot 1_0$  holds when the constraint  $V_{\text{rel}}$  is inoperative, and the variational problem is the unconstrained optimization of the energy  $H$ : Part (2) of the theorem is proved in a (ii) and a (iii).

(b)  $\alpha_{\text{rel}} \geq 2 \left[ \frac{1}{4}; 0 \right)$  and  $\alpha_{\text{rel}} = \frac{1}{2l(l+1)}$   
 At the bifurcation values of  $\alpha_{\text{rel}}$  in this regime, the following result holds,  
 as is easily ascertained:

$$\text{for } \alpha_{\text{rel}} = \frac{1}{2l(l+1)} \geq 2 \left[ \frac{1}{4}; 0 \right); l = 2, 3, \dots;$$

$$w^0 = \frac{C}{2 \frac{1}{2} \frac{1}{l(l+1)}} \stackrel{l=1}{=} \stackrel{l=2}{=} \stackrel{l=3}{=} \dots : \quad (24)$$

This proves part (3) of the theorem. QED.

## 5 Existence and properties of extremals

The final steps of the Euler-Lagrange Multiplier Method compute the value of the multiplier  $\alpha_{\text{rel}}$  by applying the fixed value of the enstrophy  $Q_{\text{rel}} > 0$ : A consequence of the completion of this circle of calculations is the determination of the physical properties of the extremal relative vorticity  $w^0$  on the basis of the relative enstrophy  $Q_{\text{rel}}$  and the spin rate  $\Omega$ : Figure 3 shows a plot of (25) and (26).

Lemma 6: The Lagrange Multipliers  $\alpha_{\text{rel}}$  of the extremals of the variational problem (10), (11) are given in terms of the spin rate  $\Omega = 0$  and the relative enstrophy  $Q_{\text{rel}} > 0$  by

$$\alpha_{\text{rel}}^+ = \frac{1}{4} \stackrel{\#}{1 + \frac{C}{Q_{\text{rel}}}} \quad (25)$$

$$\alpha_{\text{rel}}^- = \frac{1}{4} \stackrel{\#}{1 - \frac{C}{Q_{\text{rel}}}} : \quad (26)$$

Proof: Substituting the solution (22) of the Euler-Lagrange equation into the constraint in  $V_r$ ,

$$\frac{d w^0}{d \theta} = \frac{2C^2}{4 \frac{1}{2} + 2 \alpha_{\text{rel}}} = Q_{\text{rel}} > 0;$$

gives the results for  $\alpha_{\text{rel}}$ : The remaining special solutions (24) correspond to a countable set of bifurcation values. QED.

The proof of the following statement is left to the reader.

Lemma 7: (1) The first branch of solutions in Lemma 6,

$$w_{M \text{ ax}}^0 = \frac{q}{Q_{\text{rel}} \cdot 10} \quad (27)$$

corresponding to

$$\omega_{\text{rel}}^+ < \frac{1}{4};$$

are associated with solid-body rotation in the direction of spin : In terms of the original kinetic energy

$$\begin{aligned} H_{M \text{ ax}} [ \begin{smallmatrix} 10 & 10 \end{smallmatrix} ] &= 2C^2 \frac{(1 + 8 \omega_{\text{rel}}^+)^2}{16 \cdot \frac{1}{2} + 2 \omega_{\text{rel}}^+} \\ &= \frac{1}{4} Q_{\text{rel}} + \frac{1}{2} C \frac{q}{Q_{\text{rel}}}; \end{aligned} \quad (28)$$

(2) The second branch of solutions

$$w_{m \text{ in}}^0 = \frac{q}{Q_{\text{rel}} \cdot 10} \quad (29)$$

associated with

$$\begin{aligned} \omega_{\text{rel}}^2 &= \left( \frac{1}{4}; 1 \right); \\ \omega_{\text{rel}}^2 &\in \frac{1}{21(1+1)}; 1 = 2; 3; \dots \end{aligned}$$

correspond to solid-body rotation opposite the direction of spin. In this case, the original kinetic energy

$$\begin{aligned} H_{m \text{ in}} [ \begin{smallmatrix} 10 & 10 \end{smallmatrix} ] &= 2C^2 \frac{(1 + 8 \omega_{\text{rel}}^+)^2}{16 \cdot \frac{1}{2} + 2 \omega_{\text{rel}}^+} \\ &= \frac{1}{4} Q_{\text{rel}} + \frac{1}{2} C \frac{q}{Q_{\text{rel}}} \end{aligned} \quad (30)$$

for given relative enstrophy  $Q_{\text{rel}}$  and spin :

Because the Euler-Lagrange method gives only necessary conditions, to get sufficient conditions for the existence of constrained extremals, it is traditional to use the so-called Direct Method of The Calculus of Variations [19],

[18], [21], where it is shown in two parts, that (i) the unconstrained extremals of an augmented objective functional exist, and (ii) these unconstrained extremals are the constrained extremals of the original objective functional. This classical approach is presented in a sequel [22]. The approach in this paper of using the infinite dimensional geometry of the energy and relative enstrophy in manifolds, can be viewed as an alternative rigorous method for proving the existence of constrained extremals in the BVE.

The Euler-Lagrange method gives necessary conditions for extremals of a constrained problem. Sufficient conditions for the existence of extremals can nonetheless be found from the geometrical basis of the method itself. An extremal must be contained in the set of points  $p$  with common tangent spaces of the level surfaces of  $H$  and  $\Omega$ ; but only those points  $p$  where one level surface remains on the same side of the other level surface in a full neighborhood of  $p$  correspond to constrained energy maximizers or minimizers. Of those points, if moreover, the level surface of  $H$  is on the outside of the surface of  $\Omega$  in a full neighborhood of  $p_{\text{max}}$ ; with respect to the point  $p_0 = (-C; 0; \dots; 0)$  in the subspace of  $L_2(S^2)$  defined by (13), then  $p_{\text{max}}$  is a constrained energy maximum. If on the other hand, the level surface of  $H$  is on the inside of the surface of  $\Omega$  in a full neighborhood of  $p_{\text{min}}$ ; with respect to the point  $p_0 = (-C; 0; \dots; 0)$ ; then  $p_{\text{min}}$  is a constrained energy minimum.

All of the above Lemmas and Theorems form that part of variational analysis known as Necessary Conditions. We will use these facts and Lemma 3 in the proof of the following existence result which gives Sufficient Conditions for constrained extremals in terms of the geometry of the objective and constraint functionals. Figure 5 depicts case (1) in Theorem 8; figure 6 depicts case (2C) and figures 7a and 7b show the retrograde solid-body state as constrained local minimum and maximum respectively in both case (2A) and (2B).

Theorem 8: (1) The first branch of solutions  $w_{\text{max}}^0 = \frac{p}{\Omega_{\text{rel}} \sqrt{10}}$  in Lemmas 6 and 7 are global energy maximizers for any relative enstrophy  $\Omega_{\text{rel}}$  and spin :

(2) For the second branch of solutions  $w_{\text{min}}^0 = \frac{p}{\Omega_{\text{rel}} \sqrt{10}}$  in Lemmas 6 and 7, the following statements hold:

(A) If relative enstrophy is large compared to spin, i.e.,

$$\Omega_{\text{rel}} > 4^{-2} C^2 \quad (31)$$

then  $w_{\text{min}}^0$  is a special saddle point, in the sense that, it is a local energy

maxima in all eigen-directions except for  $\text{span} f_{1,1} g$ , where it is a local minimum.

(B) If relative enstrophy satisfies

$$2C^2 < Q_{\text{rel}} < 4^2 C^2 \quad (32)$$

then  $w_{\text{min}}^0$  is a constrained energy saddle point.

(C) If relative enstrophy is small compared to spin, i.e.,

$$Q_{\text{rel}} < 2C^2 \quad (33)$$

then  $w_{\text{min}}^0$  is a constrained energy minimizer.

Proof: (1) From the eigenvalues  $\lambda_m = l(l+1)$  and the fact that the spherical harmonics  $\lambda_m$  diagonalizes the energy  $H$ ; and Lemma 3 (cf. eqn. (16)), we deduce that  $H$  is positive definite in  $L_2(S^2)$ , and its level surfaces are infinite dimensional unbounded ellipsoids centered at  $p_0 = (-C; 0; \dots; 0)$ ;

with the shortest semi-major axes (of equal lengths)  $\lambda_{10}$  (cf. eqn. (16))  
in  $\text{span} f_{10}, f_{11}, f_{12}, f_{13}, \dots$ ;

and

all remaining semi-major axes (associated with azimuthal wavenumber  $l$  greater than 1)  
have lengths  $L(l)$  that are quadratic in  $l$   
and independent of the wavenumber  $m$ :

The level surfaces of relative enstrophy are non-compact concentric spheres centered at  $0$  in  $L^2(S^2)$ ;

$$\frac{\partial^2 H}{\partial p^2} = \frac{X}{\lambda_m} = \frac{2}{\lambda_m} = Q_{\text{rel}} > 0:$$

Together this implies that the level surface of  $H$  lies on the outside (wrt  $p_0$ ) of the relative enstrophy level surface for fixed  $Q_{\text{rel}}$  in a neighborhood of the point  $w_{\text{max}}^0(Q_{\text{rel}}) = +\sqrt{Q_{\text{rel}}} f_{10}$ : This proves that  $w_{\text{max}}^0(Q_{\text{rel}})$  is a global constrained energy maximizer.

(2) Using the same notation as in (1), we determine that when  $Q_{\text{rel}} < 2C^2$ , at the common point  $w_{\text{min}}^0 = -\sqrt{Q_{\text{rel}}} f_{10}$ ; the relative enstrophy hypersphere lies on the outside of the energy ellipsoid wrt  $p_0$ ; indeed both surfaces

are locally convex with respect to their respective centers. This implies that  $w_{m \text{ in}}^0$  is a constrained energy minimum in the case (33).

When  $Q_{\text{rel}} > 4^{-2}C^2$ ; it is natural to separate the common tangent space of the ellipsoid and the sphere at  $w_{m \text{ in}}^0$  into two orthogonal parts, namely,

$$(a) \text{span} f_{1;1g}; (b) \text{span} f_{1m}; l > 1g: \quad (36)$$

From the property (34) and (31), we deduce that the semi-major axes in  $\text{span} f_{10;11;1;1}$  of the energy ellipsoid at  $w_{m \text{ in}}^0$ ; have equal lengths

$$L = j \frac{q}{Q_{\text{rel}} + C} > C:$$

The enstrophy sphere at  $w_{m \text{ in}}^0$  has radii of equal lengths

$$L_{\text{rel}} = j \frac{q}{Q_{\text{rel}}} > 2C:$$

From the fact that the center of this ellipsoid is at  $p_0 = C_{10}$  while the sphere is at the origin, it follows that

$$L < L_{\text{rel}}:$$

This means that in (a)  $\text{span} f_{1;1g}$  of the common tangent space (36) at  $w_{m \text{ in}}^0$ , this ellipsoid is inside the sphere wrt  $p_0$ ; which implies that  $w_{m \text{ in}}^0$  is a local energy maximum there. And using (35), we deduce that, in the orthogonal complement, part (b) of this common tangent space (36) at  $w_{m \text{ in}}^0$ ; the ellipsoid is outside the sphere wrt  $p_0$ ; which implies that  $w_{m \text{ in}}^0$  is a local energy minimum there. Thus,  $w_{m \text{ in}}^0$  is a special saddle point in the case (31), in the sense that, apart from  $\text{span} f_{1;1g}$ , it is a local maximum.

When  $2C^2 < Q_{\text{rel}} < 4^{-2}C^2$ ; it follows from property (34) and the unboundedness property (35) of the energy ellipsoid, that there is a critical value of the azimuthal wavenumber  $l_{\text{crit}}$ ; such that in part

$$(a) \text{span} f_{1m}; l < l_{\text{crit}}g$$

of the common tangent space at  $w_{m \text{ in}}^0$ ; the ellipsoid is inside the sphere wrt  $p_0$ ; and in the orthogonal complement

$$(b) \text{span} f_{1m}; l > l_{\text{crit}}g;$$

the ellipsoid is outside the sphere wrt  $p_0$ : Thus,  $w_{m \text{ in}}^0$  is a constrained energy saddle point in the case (32). QED

## 6 Nonlinear Stability Analysis

The linear stability of the steady-states  $w_{M\text{ ax}}$  and  $w_{m\text{ in}}$  can be read off the second variation of the augmented energy functional  $E_{\text{rel}}: W$ . We are interested in proving a stronger result, namely the nonlinear or Lyapunov stability of the energy extrema. In principle this could be done using the geometric (convexity) properties of the relative enstrophy and energy manifolds, recalling that the former is a sphere in  $L^2(S^2)$  and the latter is an "ellipsoid" in the same Hilbert space. Due to the infinite-dimensionality of  $L^2(S^2)$ , and the consequent non-compactness of the enstrophy manifold, this is a delicate undertaking.

Instead, we propose to follow the method discussed in detail in [16], [10], [11], and also in [2], [?]. The first step consists of the identification of two quadratic functionals  $Q_1$  and  $Q_2$  in the perturbation  $w$  such that

$$\begin{aligned} Q_1(w) &= H[w_{M\text{ ax}} + w] - H[w_{M\text{ ax}}] - D_{M\text{ ax}}w \\ Q_2(w) &= [w_{M\text{ ax}} + w] - [w_{M\text{ ax}}] - D_{M\text{ ax}}w \end{aligned}$$

Let  $f_{\text{Im}} g$  denote the perturbation Fourier coefficient based on the steady-state  $w_{M\text{ ax}} = \frac{1}{\sqrt{Q_{\text{rel}}}} \mathbf{1}_{10}$ ; that is, the steady state is given by

$$\begin{aligned} \mathbf{1}_{10}(w_{M\text{ ax}}) &= \frac{q}{Q_{\text{rel}}}; \\ \mathbf{1}_{\text{Im}}(w_{M\text{ ax}}) &= 0 \text{ for all other modes.} \end{aligned}$$

It is natural and convenient to choose the positive definite quadratic forms

$$\begin{aligned} Q_1(f_{\text{Im}} g) &= H[w_{M\text{ ax}} + w] - H[w_{M\text{ ax}}] - D_{M\text{ ax}}w \\ &= -\frac{1}{4} \sum_{\substack{1 \leq m \leq 10 \\ m \neq 10}} \frac{1}{2} \frac{x_m^2}{\lambda_m} - 0; \\ Q_2(f_{\text{Im}} g) &= \sum_{m \neq 10} \frac{x_m^2}{\lambda_m} - 0; \end{aligned}$$

Then,  $Q_1 + Q_2$  is positive definite, and is clearly a norm for the perturbation  $w$  since  $Q_2(w) = \|w\|_2^2$ :

From the fact that at steady-state  $w_{M\text{ ax}}; D(H + \lambda)(w_{M\text{ ax}}) - w = 0$ ; it follows that

$$\begin{aligned} (Q_1 + Q_2)(f_{\text{Im}}(t)g) &= (H + \lambda)[w_{M\text{ ax}} + w(t)] - (H + \lambda)[w_{M\text{ ax}}] \\ &= (H + \lambda)[w_{M\text{ ax}} + w(0)] - (H + \lambda)[w_{M\text{ ax}}] \\ &= E(0) - 0; \end{aligned}$$

that is, the sum  $Q_1 + Q_2$  is conserved along trajectories of the BVE. Thus, we conclude that trajectories that start near  $w_{M\text{ ax}}$  will remain nearby for all time, that is,  $w_{M\text{ ax}}$  has been shown to be Lyapunov stable.

The same arguments go through for the energy minimizer  $w_{m\text{ in}}$  when the relative enstrophy  $Q_{\text{rel}} < 2C^2$ : And for the saddle point  $w_{m\text{ in}}$  when  $Q_{\text{rel}} > 4^2C^2$ ; a modified argument where perturbations are restricted to be in the orthogonal complement of  $\text{span} f_{10, 1, 1g}$  in  $L^2(S^2)$ , proves that  $w_{m\text{ in}}$  has some degree of nonlinear stability. This completes the proof of

**Theorem 9:** The global energy maximizer  $w_{M\text{ ax}}$  is Lyapunov stable in the BVE under all conditions of spin, energy and relative enstrophy. The constrained energy minimizer  $w_{m\text{ in}}$  is Lyapunov stable in the BVE in the low energy, low enstrophy regime, that is, when  $Q_{\text{rel}} < 2C^2$ : If  $Q_{\text{rel}} > 4^2C^2$  (high enstrophy, high energy regime), then the saddle point  $w_{m\text{ in}}$  is nonlinearly stable to all perturbations with azimuthal wavenumber 1–2: In the intermediate regime,  $2C^2 < Q_{\text{rel}} < 4^2C^2$ ;  $w_{m\text{ in}}$  is unstable.

## 7 Discussion and conclusions

From the point of view of applications to planetary atmospheres, the physical consequences of theorems 5, 8 and 9 is embodied in the following over-arching statement:

There is a relative enstrophy threshold value  $2C^2$  such that below it, the constrained energy extrema consist of the counter-rotating local energy minimizer state  $w_{m\text{ in}}^0 = \frac{p}{Q_{\text{rel}}} \mathbf{e}_{10}$  and the pro-rotating global energy maximizer state  $w_{M\text{ ax}}^0 = +\frac{p}{Q_{\text{rel}}} \mathbf{e}_{10}$ . When relative enstrophy exceeds this value, the pro-rotating global energy maximizer state  $w_{M\text{ ax}}^0 = +\frac{p}{Q_{\text{rel}}} \mathbf{e}_{10}$  persists but the counter-rotating state  $w_{m\text{ in}}^0$  becomes a constrained saddle point.

In other words, the counter-rotating state is a nonlinearly stable energy extremum only for low relative enstrophy and low kinetic energy. The nonlinearly stable counter-rotating steady state  $w_{m\text{ in}}^0 = \frac{p}{Q_{\text{rel}}} \mathbf{e}_{10}$  changes stability to a constrained saddle point via a saddle-node bifurcation when the rate of spin decreases past the threshold value

$$\circ = \frac{p}{C} \frac{\overline{Q_{\text{rel}}}}{\overline{Q_{\text{rel}}}_{10}};$$

with relative enstrophy fixed at  $Q_{\text{rel}}$ : When the relative enstrophy is large enough compared to the spin rate  $\circ > 0$ , that is,  $Q_{\text{rel}} > 2C^2$ , the only

nonlinearly stable steady state in the BVE model is the global energy maximizer  $w_{\text{max}}^0 = \frac{P}{Q_{\text{rel}}} \approx 10$ ; with the caveat that for  $Q_{\text{rel}} > 4^{-2}C^2$ ; the counter-rotating state  $w_{\text{min}}^0$  is nonlinearly stable to zonally-symmetric perturbations.

Thus, for any relative enstrophy and any given spin rate  $\sigma > 0$ ; a super-rotational Lyapunov stable steady state exists in the BVE. When  $Q_{\text{rel}} < 4^{-2}C^2$ ; both the global energy maximizer and global energy minimizer are Lyapunov stable solid-body rotational states.

In comparison, numerical simulations of the terrestrial General Circulation Model (GCM) show that super (sub)-rotational flows behave like saturated asymptotic steady states of a complex dam-ped driven system (cf. [12] and ref. therein). The super-rotating state appears to be associated only with sufficiently energetic flows in these numerically intensive simulations. Moreover, the basin of attraction of these flows can be reasonably characterized by only a few initial quantities such as energy and angular momentum, and the super (sub)-rotational end states appear to be quite robust in a numerical sense. The super-rotational state is taken to be the one where the fluid's relative angular momentum is in the direction of the planet's spin. The vertically averaged barotropic component in a dam-ped driven multi-layered atmospheric system therefore have asymptotic quasi-steady states which are super and sub-rotational states near to the basic zonal states [12], [4]. Recent numerics (cf. [12] and references therein) confirm the super-rotational state is more relevant to the atmosphere of Venus and is associated only with sufficiently high kinetic energy; the sub-rotational state arises only for lower energies in for instance, the atmosphere of Titan [12].

A more direct comparison can be made between our detailed results and those reported by Yoden and Yamada. In particular, they found robust relaxation to a prograde solid-body state for small to intermediate values of the planetary spin. The first is consistent with our first prediction that the prograde solid-body state arises only when the kinetic energy of the flow is high enough relative to the planetary spin, or equivalently, for a given range of kinetic energy, it is allowed only for relatively small planetary spins. The second is partially consistent with our second prediction that the retrograde solid-body state is nonlinearly stable only for planetary spins that are large in comparison to the relative enstrophy, if one allows for the fact that the large anticyclonic polar vortex state is a superposition of mainly the retrograde solid-body state and some zonally-symmetric spherical harmonics with wavenumber  $l < 5$ .

Figure 1: Graph of energy  $H$  vs. coordinates  $k = \omega_{10}$  of extremes as in (17).

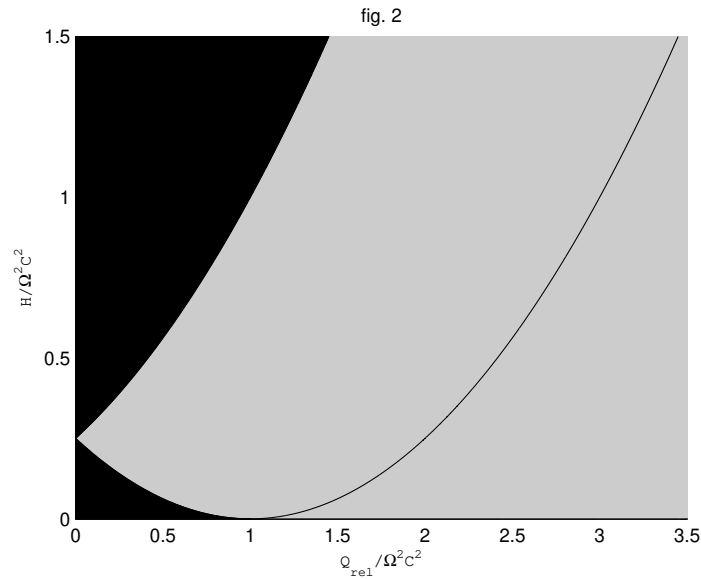
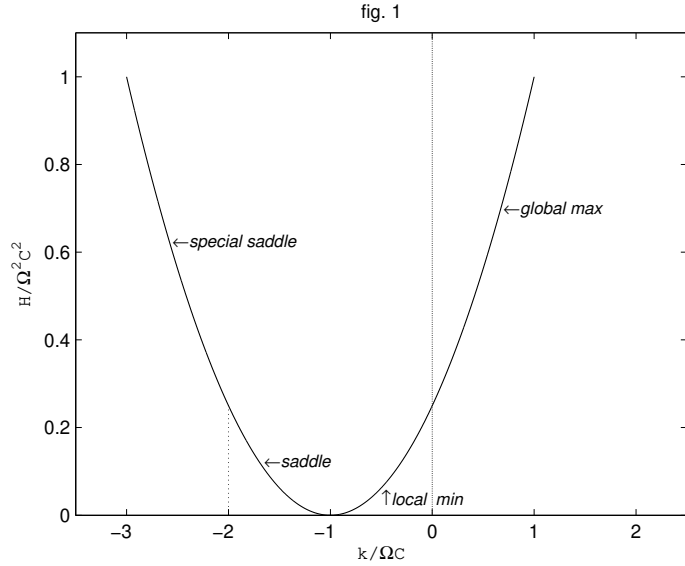


Figure 2: Energy  $H$  – relative enstrophy  $\Omega_{\text{rel}}$  space; black region denotes unpermittted values; gray region denotes non-extremal permitted values; curves denote values at extremes as in (18).

Figure 3: Graph of Lagrange Multipliers  $\lambda_{\text{rel}}$  vs. square-root of relative enstrophy,  $\Omega_{\text{rel}}^{1/2}$  for fixed spin  $\sigma > 0$  as in (25) and (26).

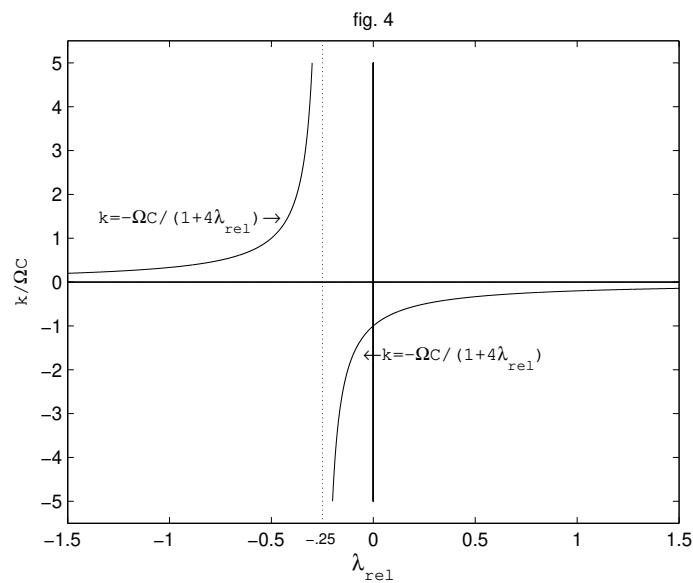
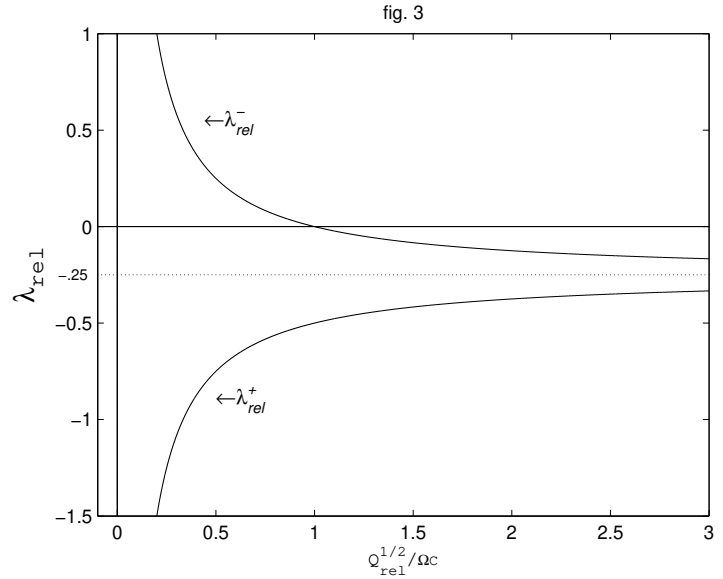


Figure 4: Graph of extremal coordinates  $k$  vs. Lagrange Multipliers  $\lambda_{\text{rel}}$  for fixed spin  $\sigma > 0$  as in (22) and (23).

Figure 5: Projections of energy ellipsoid and enstrophy sphere showing the common tangent at global maximum  $w_{\text{Max}}^0$  when energy exceeds  $H_c$ .

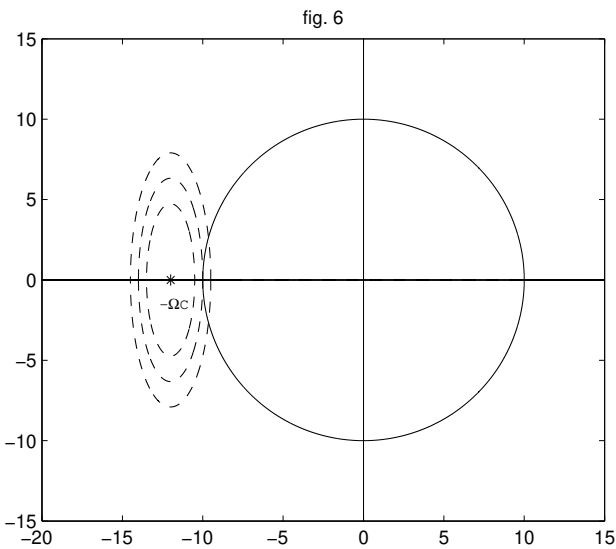
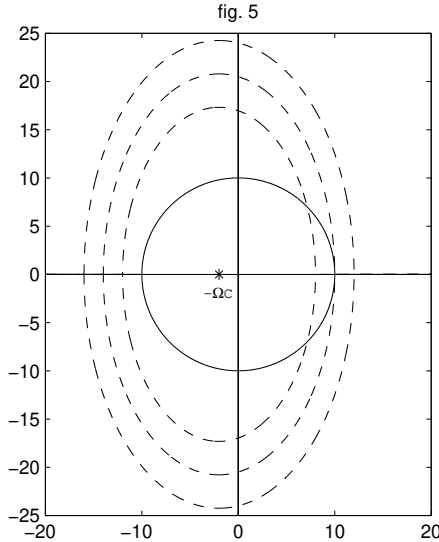
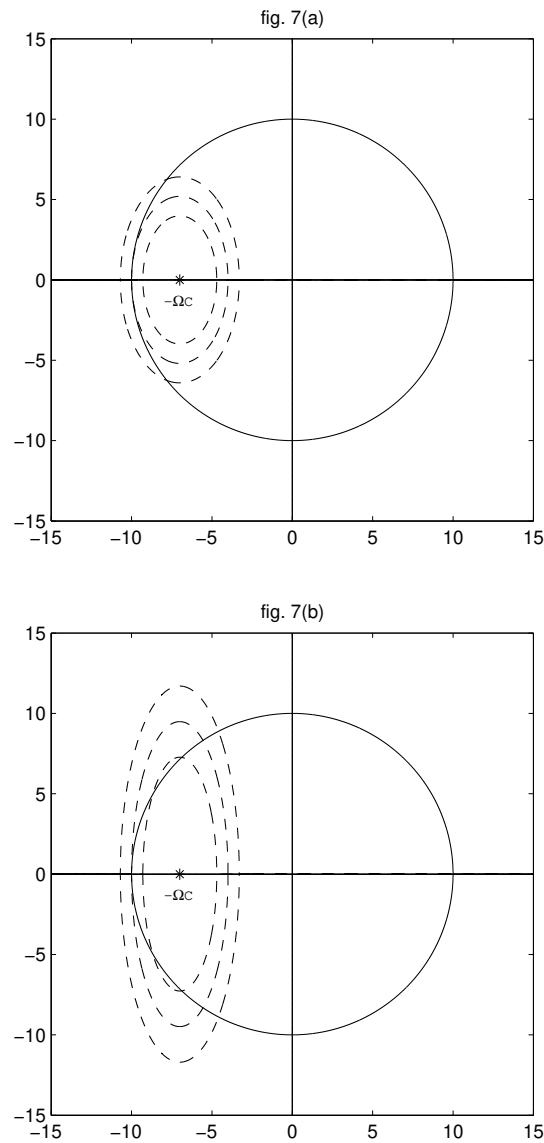


Figure 6: Projections of energy ellipsoid and enstrophy sphere showing the common tangent at local minimum  $w_{\text{min}}^0$  when (33) holds.

Figure 7: (a) Projections of energy ellipsoid and enstrophy sphere showing the saddle point  $w_m^0$  as local minimum when (32) or (31) holds; (b) Projections of energy ellipsoid and enstrophy sphere showing the saddle point  $w_m^0$  as local maximum



## References

- [1] T. G. Shepherd, Non-ergodicity of inviscid two-dimensional flow on a beta-plane and on the surface of a rotating sphere, *J. Fluid Mech.*, 184, 289–302, 1987.
- [2] M. Mu and T. G. Shepherd, On Arnold's second nonlinear stability theorem for two-dimensional quasi-geostrophic flow, *Geophys. Astrophys. Fluid Dyn.* 75 21–37.
- [3] J. Cho and L. Polvani, The emergence of jets and vortices in freely evolving, shallow-water turbulence on a sphere, *Phys. Fluids* 8 (6), 1531–1552, 1995.
- [4] S. Yoden and M. Yamada, A numerical experiment on 2D decaying turbulence on a rotating sphere, *J. Atmos. Sci.*, 50, 631, 1993.
- [5] C. Foias and R. Saut, Indiana U. Math Journ 33, 457 –, 1984.
- [6] R. Fjorhoff, Application of integral theorems in deriving criteria of stability for laminar flows and for the baroclinic circular vortex, *Geophys. Publ.* 17 (6), 1, 1950.
- [7] R. Fjorhoff, On the changes in the spectral distribution of kinetic energy for 2D non-divergent flows, *Tellus*, 5, 225 – 230, 1953.
- [8] C. Leith, Minimum enstrophy vortices, *Phys. Fluids*, 27, 1388 – 1395, 1984.
- [9] D. W. Moore and T. G. Shepherd, On the existence of 2D Euler flows satisfying energy-Casimir criteria, *Phys. Fluids* 12, 727, 2000.
- [10] V. I. Arnold, Conditions for nonlinear stability of stationary plane curvilinear flows of an ideal fluid, *Sov. Math. Dokl.*, 6, 773–777, 1965.
- [11] V. I. Arnold, On an a priori estimate in the theory of hydrodynamic stability, *AM S Translations, Ser. 2*, 79, 267–269, 1969.
- [12] A. Del Genio, W. Zhuo and T. Eichler, Equatorial Superrotation in a slowly rotating GM: implications for Titan and Venus, *Icarus* 101, 1–17, 1993.

- [13] S.J.Chem, Math Theory of the Barotropic Model in GFD , PhD thesis, Cornell University, 1991.
- [14] R.H.Kraichnan, Statistical dynamics of two-dimensional flows, *J. Fluid Mech.* 67, 155-175, 1975.
- [15] C.C.Lim, Energy maximizers and robust symmetry breaking in vortex dynamics on a non-rotating sphere, *SIAM J. Applied Math.*, 2005, formally accepted for publication (galley stage).
- [16] D.Holm, J.Marsden, T.Ratiu and A.Winstein, Nonlinear stability of uid and plasma equilibria, *Physics Report* 123, 1-116, 1985.
- [17] P.B.Rhines, Waves and turbulence on a beta plane, *J. Fluid Mech.*, 69 (3), 417-443, 1975.
- [18] I.Ekeland and R.Temam, *Convex Analysis and Variational Problems*, North-Holland, 1976.
- [19] D.Smith, *Variational Methods in Optimization*, Dover
- [20] K.K.Tung, Barotropic instability of zonal flows, *J. Atmos. Sc.*, 38, 308 - 321, 1981.
- [21] P.D.Lax, *Functional Analysis*, Wiley-Interscience, 2002.
- [22] C.C.Lim and Junping Shi, The role of higher vorticity moments in a variational formulation of a Barotropic Vorticity Model on the rotating sphere, submitted 2005.

List of Figure Captions:

Figure 1. Graph of energy  $H$  vs. coordinates  $k = \sqrt{10}$  of extrema as in (17).

Figure 2. Energy  $H$  – relative enstrophy  $Q_{\text{rel}}$  space; black region denotes unperturbed values; gray region denotes non-extremal perturbed values; curves denote values at extrema as in (18).

Figure 3. Graph of Lagrange Multipliers  $\lambda_{\text{rel}}$  vs. square-root of relative enstrophy,  $Q_{\text{rel}}$  for fixed spin  $> 0$  as in (25) and (26).

Figure 4. Graph of extremal coordinates  $k$  vs. Lagrange Multipliers  $\lambda_{\text{rel}}$  for fixed spin  $> 0$  as in (22) and (23).

Figure 5. Projections of energy ellipsoid and enstrophy sphere showing the common tangent at global maximum  $w_{\text{max}}^0$  when energy exceeds  $H_c$ .

Figure 6. Projections of energy ellipsoid and enstrophy sphere showing the common tangent at local minimum  $w_{\text{min}}^0$  when (33) holds.

Figure 7a. Projections of energy ellipsoid and enstrophy sphere showing the saddle point  $w_{\text{min}}^0$  as local minimum when (32) or (31) holds.

Figure 7b. Projections of energy ellipsoid and enstrophy sphere showing the saddle point  $w_{\text{min}}^0$  as local maximum.